A method to estimate the influence of the notch-root radius on the fracture toughness measurement of ceramics

David Picard, Dominique Leguillon, Claude Putot

A method to estimate the influence of the notch-root radius on the fracture toughness measurement of ceramics

D. Picard[a], D. Leguillon[b,*], C. Putot[a]

[a]IFP, Dept. de Mécanique Appliquée, Rueil-Malmaison, France

[b]Laboratoire de Modélisation en Mécanique, CNRS UMR7607, Université P. et M. Curie, Paris, France

The fracture toughness measurement of ceramics is based on notched specimens. If the notch-root radius is too large, it leads to overestimate the actual fracture toughness of the material. It is then necessary to control the notch shape and to machine it carefully in order to have a root-radius small enough (<10 μm) to be below the sensitivity threshold of the material. Then, the notch confounds with a sharp crack. Alternatively, it is proposed in this work to bring a correction to the measured fracture toughness depending on the notch-root radius. No restriction is brought to this radius except that it must be small compared to the notch length.

Keywords: Mechanical properties; Fracture; Strength; Toughness and toughening; Notched specimen; Testing

1. Introduction

The fracture toughness is the capacity of resistance of a material to a crack growth. Whatever the method used, its measurement requires in general a pre-existing sharp crack within the specimen. In many cases, it is obtained simply by a saw cut. Sometimes it is followed by a fatigue loading. But, in any case the geometry of this sharp crack is difficult to control, if not impossible in ceramics. If the notch-root radius is too large, it leads to overestimate the actual fracture toughness of the material. A rough estimation of the initial fatigue crack length can also be a cause of inaccuracy.

An alternative method called SENB-S is proposed.[1–3] It relies on 3-point bending notched specimens and consists in controlling the notch-root radius ρ of the saw cut estimated to be one half of the saw cut thickness e (Fig. 1). Reliable measures are obtained if the notch is machined very precisely, leading to a radius smaller than a critical threshold.[1,2] This bound can be empirically determined according to the microstructure of the material and especially to the grain size. In the present analysis no restriction is brought to the notch-root radius, the only assumption is that it must be small compared to the saw cut length. It is then necessary to bring a correction to the apparent measured fracture toughness of the material to get the actual value. It depends of course on the blunting caused by the rounding. It is determined herein using simultaneously two fracture criteria: an energy and a stress condition. It requires in addition the knowledge of the material strength.

The analysis is based on matched asymptotics, the small parameter being the saw cut thickness. The elastic solution of the 3-point bending problem, or any other kind of loading, is approximated by a far and a near field. The far field is a rough approximation where the notch is modelled by a thin crack, allowing the definition of an apparent fracture toughness based on the stress intensity factor at the crack tip. The near field zooms in the vicinity of the rounded end of the notch, providing an accurate stress field closed to the notch root. In this second framework no stress intensity factor can be invoked. To be consistent, these two fields must match in an intermediate area.

A similar analysis was carried out previously for v-notched specimens,[4] but the method used there could not

* Corresponding author. Tel.: +33 144 275 322; fax: +33 144 275 259.
E-mail address: dol@ccr.jussieu.fr (D. Leguillon).

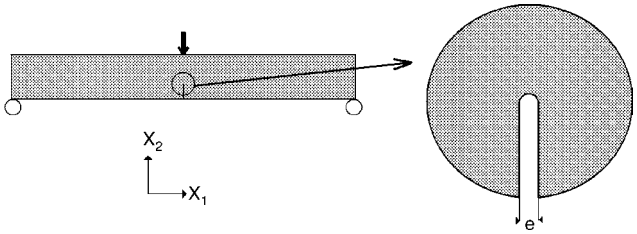

Fig. 1. The 3-point bending specimen, e is the saw cut thickness, the notch-root radius is estimated to be $\rho = e/2$.

be extended in a straightforward manner to the present geometry.

2. Asymptotic analysis of the undamaged specimen

The analysis is based on a two-scale asymptotic analysis in plane strain linear elasticity. The actual displacement field is denoted $\underline{U}^e$, the index e being used to recall its dependence on the saw cut thickness. It is solution to the following set of equations:

$$\begin{cases} -\nabla \cdot \sigma = 0 \\ \sigma = C : \nabla \underline{U}^e \\ \sigma \cdot \underline{n} = O \text{ along the saw cut faces} \\ +\text{remote boundary conditions} \end{cases} \tag{1}$$

The first equation is the balance of momentum (equilibrium), σ denotes the stress tensor. The symbol nabla ∇ holds for derivatives with respect to the Cartesian coordinates x_1 and x_2. The second equation is the constitutive law, C is the elastic operator relying classically on the Young's modulus E (MPa) and the Poisson's ratio ν of the material. The third equation expresses that the saw cut faces are free of traction. The remote boundary conditions do not play an important role in the analysis.

In a first step, assuming that e is small compared to the saw cut length, the actual solution is approximated by:

$$\underline{U}^e(x_1, x_2) = \underline{U}^0(x_1, x_2) + \text{small correction} \tag{2}$$

The first term $\underline{U}^0$ is solution to an idealized problem with an infinitely thin cut (the index 0 means $e = 0$), i.e. a perfectly sharp crack. It is illustrated on Fig. 1 (left). The small correction in (2) decreases to 0 as $e \to 0$. Obviously this approximation is valid except in a vicinity of the saw cut where it becomes meaningless. It is so-called the far field or the outer field. It undergoes the classical singularity at the crack tip:

$$\underline{U}^0(x_1, x_2) = \underline{U}^0(0, 0) + k_{\mathrm{I}}\sqrt{r}\,\underline{u}^{\mathrm{I}}(\theta) + \cdots \tag{3}$$

where r and θ stand for the polar coordinates with the origin at the crack tip. The first term of the expansion in (3) is present for consistency, it is the irrelevant rigid translation of the origin. The coefficient k_{I} (MPa m$^{1/2}$) is the usual opening mode I stress intensity factor. Because of the symmetries, the antisymmetric mode II is not activated in a 3-point bending experiment.

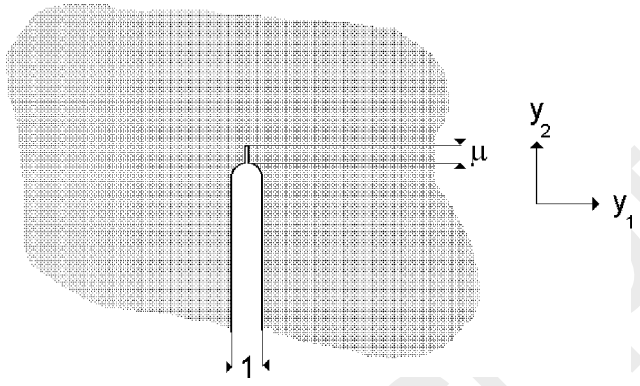

Fig. 2. The notch-root vicinity with a short new crack embedded in the unbounded inner domain (stretched domain).

It is emphasized that k_{I} is an apparent stress intensity factor since it corresponds to a simplified geometry of the saw cut. No actual intensity factor exists at the root of a rounded notch. It corresponds to the quantity extracted from experiments, using notched beam formulas.[2]

To have a detailed form of the actual solution $\underline{U}^e$, the initial domain is stretched by $1/e$. The new dimensionless space variables are $y_i = x_i/e$ $(i = 1, 2)$. As $e \to 0$ the corresponding domain becomes unbounded, it is illustrated on Fig. 2. There is an infinitely long saw cut (dimensionless thickness 1) and the outer boundary is sent to infinity. This so-called inner domain ignores the exact geometry of the specimen. The actual solution is assumed to expand in the following way:

$$\begin{aligned} \underline{U}^e(x_1, x_2) &= \underline{U}^e(ey_1, ey_2) \\ &= F_0(e)\underline{V}^0(y_1, y_2) + F_1(e)\underline{V}^1(y_1, y_2) + \cdots \end{aligned} \tag{4}$$

with

$$\lim_{e\to 0}\left[\frac{F_1(e)}{F_0(e)}\right] = 0$$

The $\underline{V}^i$'s are solutions to problems with prescribed behaviour at infinity, they form the near or inner field. More precisely, these terms must match at infinity with the behaviour of the far field near the singular point as described in (3), in order to have consistent far and near (outer and inner) representations of the solution. It means that there exists an intermediate area in which the two expansions (2) and (4) hold true. Eq. (4) together with (3) leads to[5]:

$$F_0(e) = 1; \quad \underline{V}^0(y_1 y_2) = \underline{U}^0(0, 0); \quad F_1(e) = k_{\mathrm{I}}\sqrt{e};$$
$$\underline{V}^1(y_1, y_2) \approx \sqrt{\gamma}\,\underline{u}^{\mathrm{I}}(\theta)$$

Here, $\gamma = r/e$ and the symbol $\approx$ holds for "behaves like — at infinity". As before in (3), the first term is irrelevant. Using the superposition principle:

$$\underline{V}^1(y_1, y_2) = \sqrt{\gamma}\underline{u}^{\mathrm{I}}(\theta) + \hat{\underline{V}}^1(y_1, y_2)$$

where $\hat{\underline{V}}^1$ is solution to a problem derived from (1) and expressed in the stretched dimensionless variables y_1 and y_2:

$$\begin{cases} -\nabla_y \cdot \hat{\sigma} = 0 \\ \hat{\sigma} = C : \nabla_y \hat{\underline{V}}^1 \\ \hat{\sigma} \cdot \underline{n} = -\sigma^{\mathrm{I}} \cdot \underline{n} \ \text{ along the saw cut faces} \\ \hat{\underline{V}}^1 \ \text{ decreases to 0 at infinity} \end{cases} \tag{5}$$

with

$$\sigma^{\mathrm{I}} = C : \nabla_y[\sqrt{\gamma}\underline{u}^{\mathrm{I}}(\theta)]$$

The symbol nabla ∇_y holds for derivatives with respect to y_1 and y_2. The third equation expresses once again that the saw cut faces are free of traction. The last one is the matching condition resulting of the superposition principle. The debatable point relies on the third equation but it is proved that[6]:

$$\int_{\Sigma} \sigma^{\mathrm{I}} \cdot \underline{n} \, \mathrm{d}s = 0$$

where Σ denotes the stretched saw cut faces. It ensures the problem in (5) to be well-posed, since the resulting moment also vanishes due to the symmetries of the singular term.

The expansion finally writes:

$$\begin{aligned} \underline{U}^e(x_1, x_2) &= \underline{U}^e(ey_1, ey_2) \\ &= \underline{U}^0(0,0) + k_{\mathrm{I}}\sqrt{e}\,[\sqrt{\gamma}\underline{u}^{\mathrm{I}}(\theta) + \hat{\underline{V}}^1(y_1, y_2)] + \cdots \end{aligned} \tag{6}$$

The function $\hat{\underline{V}}^1$ is independent of the applied load and of the geometry of the specimen. They intervene in (6) through the single parameter k_{I}.

3. Asymptotic analysis of the damaged specimen including a short crack

Let us now consider a small crack emanating from the notch root (Fig. 2). It is assumed that its length ℓ is smaller or of the same order of magnitude than the saw cut thickness e:

$$\ell = \mu e \quad \text{and} \quad \mu < +\infty$$

By analogy, the actual solution with the additional crack expands as (see (6)):

$$\begin{aligned} \underline{U}^e(x_1, x_2, \ell) &= \underline{U}^e(ey_1, ey_2, e\mu) \\ &= \underline{U}^0(0,0) + k_{\mathrm{I}}\sqrt{e}[\sqrt{\gamma}\underline{u}^{\mathrm{I}}(\theta) + \hat{\underline{V}}^1(y_1, y_2, \mu)] + \ldots \end{aligned} \tag{7}$$

The term $\hat{\underline{V}}^1$ now depends on the dimensionless crack length μ, it fulfils the same system of equation than the previous $\hat{\underline{V}}^1$ (in (5)) and the additional condition that the new crack faces are also free of traction. To have homogeneous notations we rewrite:

$$\hat{\underline{V}}^1(y_1, y_2) = \hat{\underline{V}}^1(y_1, y_2, 0)$$

Note that the unbounded inner domain makes impossible the direct computation of the functions $\hat{\underline{V}}^1$. An approximation is obtained by artificially bounding the domain at a large distance R^∞ (large compared to μ and to 1, i.e. the stretched saw cut thickness, say $R^\infty = 400$). The vanishing condition at infinity is written out prescribing either a Neumann or a Dirichlet boundary condition on the virtual line Γ^∞:

$$\hat{\sigma} \cdot \underline{n} = 0 \quad \text{or} \quad \hat{\underline{V}}^1 = 0 \ \text{ on } \ \Gamma^\infty$$

It replaces in (5) the last equation describing the behaviour at infinity providing a classical boundary value problem.

4. The energy release rate

The following energy balance must hold true:

$$\delta W_{\mathrm{p}} + \delta W_{\mathrm{k}} + G_{\mathrm{c}}\delta S = 0$$

The first term δW_{p} is the change in potential energy between the initial state prior to any crack onset and the final state embedding a new short crack (length ℓ) at the notch root (Fig. 2). The second one δW_{k} is the change in kinetic energy and the last one is the fracture energy. This latter is proportional to the newly created crack surface δS, the scaling coefficient being the material fracture toughness G_{c} ($\mathrm{J\,m^{-2}}$). Since $\delta W_{\mathrm{k}} \geq 0$, the above condition leads to the Griffith criterion:

$$-\frac{\delta W_{\mathrm{p}}}{\delta S} \geq G_{\mathrm{c}} \tag{8}$$

The left hand side ratio is called the energy release rate G.

The change in potential energy can be expressed as[4,5]:

$$-\delta W_{\mathrm{p}} = \Psi(\underline{U}^e(x_1, x_2, \ell), \underline{U}^e(x_1, x_2, 0)) \tag{9}$$

Ψ is a contour integral relying on the Betti's theorem. For any displacement fields $\underline{W}^1$ and $\underline{W}^2$ satisfying the equilibrium equations, it is defined by:

$$\Psi(\underline{W}^1, \underline{W}^2) = \frac{1}{2}\int_{\Gamma} [\sigma(\underline{W}^1) \cdot \underline{n} \cdot \underline{W}^2 - \sigma(\underline{W}^2) \cdot \underline{n} \cdot \underline{W}^1] \, \mathrm{d}s \tag{10}$$

The stress fields involved in (10) relate to the displacement fields through the constitutive law:

$$\sigma(\underline{W}^i) = C : \nabla_y \underline{W}^i$$

The integral in (10) is independent of the contour Γ starting and finishing on the faces of the notch. For technical reasons, the contour in (10) must be taken as large as possible within the artificially bounded inner domain (see the end of Section 3).

Using now the asymptotics (6) and (7) in (9), it writes

$$-\delta W_{\mathrm{p}} = k_{\mathrm{I}}^2 e \frac{A(\mu) - A(0)}{E^*} d + \cdots \quad \text{with} \quad E^* = \frac{E}{1-\nu^2} \tag{11}$$

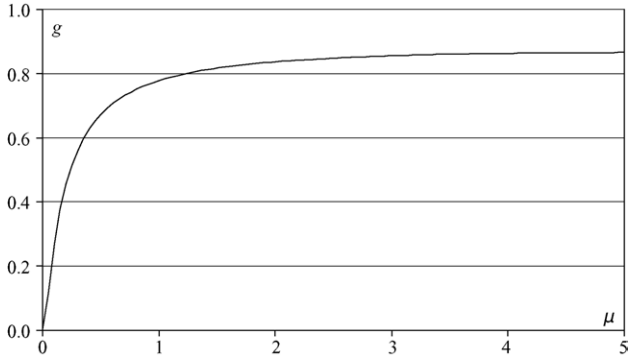

Fig. 3. The dimensionless function $g(\mu)$ (13) vs. the dimensionless crack extension length μ.

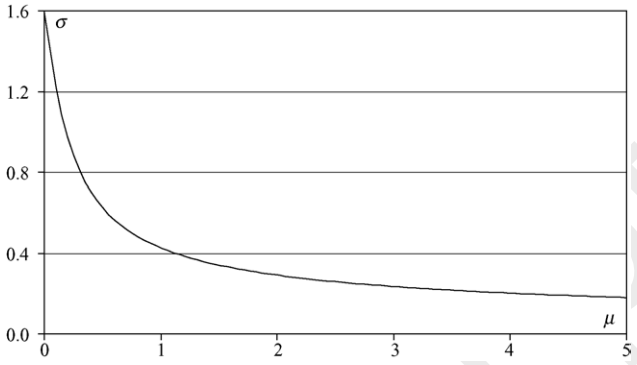

Fig. 4. The dimensionless tension $\tilde{\sigma}_t(\mu)$ (16) acting ahead of the notch root prior to any crack onset, vs. the dimensionless distance μ to the notch root.

where d is the specimen thickness (plane elasticity). The dimensionless coefficients A (either for $\mu \neq 0$ or $\mu = 0$) are defined by[5]:

$$A(\mu) = E^* \Psi(\hat{\underline{V}}^1(y_1, y_2, \mu), \sqrt{\gamma}\underline{u}^{\mathrm{I}}(\theta))$$

The newly created crack surface is:

$$\delta S = \ell d$$

and then the above criterion (8) rewrites, thanks to (11):

$$k_{\mathrm{I}}^2 \frac{A(\mu) - A(0)}{\mu E^*} \geq G_{\mathrm{c}} \tag{12}$$

The energy release rate can be expressed in terms of the dimensionless function $g(\mu)$:

$$G = \frac{g(\mu)}{E^*} k_{\mathrm{I}}^2 \quad \text{with} \quad g(\mu) = \frac{A(\mu) - A(0)}{\mu} \tag{13}$$

It is a generalization of the Irwin formula (see also (17) below) and $g(\mu) \to 1$ as $\mu \to \infty$ (Fig. 3). Obviously, as μ increases the new crack becomes longer and longer and the saw cut lengthened by the new crack behaves more and more like a long crack.

The function $g(\mu)$ is independent of the Young's modulus E, but it cannot be proved that it is independent of the Poissons's ratio ν, even if the coefficient $1 - \nu^2$ has been singled out. Fig. 3 is plotted for $\nu = 0.3$. Nevertheless, different values of ν ranging in a usual domain (i.e. from 0.1 to 0.4) have been checked, they give almost confounded curves.

5. The failure criterion

Indeed, the inequality (12) is an incremental form of the Griffith criterion, the dimensionless crack extension length μ is still unknown. Usually, taking the limit for $\delta S \to 0$ (i.e. $\ell \to 0$) in (8) overcomes this difficulty. It leads to the classical definition of the energy release rate:

$$G^{\mathrm{diff}} = \lim_{\delta S \to 0} \left(-\frac{\delta W_{\mathrm{p}}}{\delta S} \right) = -\frac{\partial W_{\mathrm{p}}}{\partial S}$$

G^{diff} is the derivative of the potential energy with respect to the crack surface (up to the sign). It is effective in the analysis of the growth of a pre-existing crack but leads to some paradox in many other cases as the present one. Here, this differential form G^{diff} vanishes whatever the applied load and then can never become larger or equal to the fracture toughness G_{c}, no failure can be predicted. The main explanation is that the condition (8) is necessary for fracture but not sufficient, except for a sharp crack. Various experiments show that in general a stress condition must also be accounted for.[7]

Let us denote by $\sigma_t(\ell)$ the tension acting at a distance ℓ on the ligament ahead of the notch root prior to any crack onset. By symmetry, it is the only relevant stress component. It is a decreasing function of the distance to the notch root (Fig. 4). The additional stress condition is that this tension must exceed the material strength σ_{c} all along the putative crack path, then:

$$\sigma_t(\ell) \geq \sigma_{\mathrm{c}}$$

According to the expansion (6) (i.e. the approximation of the actual solution prior to the crack onset), the above stress condition rewrites:

$$\frac{k_{\mathrm{I}}}{\sqrt{e}} [(\sigma_t^{\mathrm{I}}(\mu) + \hat{\sigma}_t(\mu)] \geq \sigma_{\mathrm{c}} \tag{14}$$

For a fixed k_{I}, i.e. for a fixed applied load, the inequality (12) gives a lower bound of the admissible dimensionless crack extension lengths μ while (14) gives an upper bound. The compatibility between these two bounds provides the critical length μ_{c} (and $\ell_{\mathrm{c}} = \mu_{\mathrm{c}} e$) for which the two conditions (12) and (14) are simultaneously fulfilled. The critical value μ_{c} is solution to the following equation:

$$\frac{g(\mu_{\mathrm{c}})}{E^* \tilde{\sigma}_t(\mu_{\mathrm{c}})^2} = \frac{G_{\mathrm{c}}}{\sigma_{\mathrm{c}}^2 e} \tag{15}$$

with

$$\tilde{\sigma}_t(\mu_{\mathrm{c}}) = \sigma_t^{\mathrm{I}}(\mu_{\mathrm{c}}) + \hat{\sigma}_t(\mu_{\mathrm{c}}) \tag{16}$$

The function $\tilde{\sigma}_t(\mu)$ is plotted in Fig. 4 for $\nu = 0.3$. But once again it has been checked that the Poisson's ratio plays a

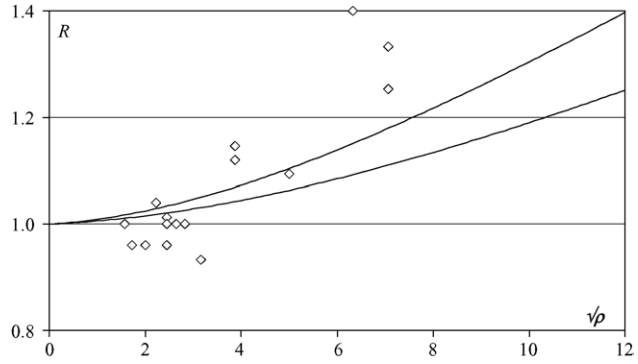

Fig. 5. The ratio $R = k_{\mathrm{Ic}}^{\mathrm{app}}/k_{\mathrm{Ic}}$ vs. the square root of the notch-root radius $\sqrt{\rho}$ ($\mu\mathrm{m}^{1/2}$) for alumina. Diamonds: experiments,[1] solid lines: prediction (20).

minor role. Different values of ν ranging from 0.1 to 0.4 give almost confounded curves.

Using the Irwin formula:

$$G_{\mathrm{c}} = \frac{1}{E^*} k_{\mathrm{Ic}}^2 \tag{17}$$

where k_{Ic} (MPa $\mathrm{m}^{1/2}$) is the critical value of the mode I stress intensity factor, also baptised toughness because of its obvious one to one relationship with G_{c}, the Eq. (15) becomes dimensionless:

$$\frac{g(\mu_{\mathrm{c}})}{\tilde{\sigma}_t(\mu_{\mathrm{c}})^2} = \frac{1}{e}\frac{k_{\mathrm{Ic}}^2}{\sigma_{\mathrm{c}}^2} \tag{18}$$

The dimensionless critical length μ_{c} is a function of the saw cut thickness e and of the material fracture parameters occurring in the right hand side term of the above equation.

The failure criterion involves the apparent stress intensity factor k_{I} and using either (12) or (14), it finally reads:

$$k_{\mathrm{I}} \geq k_{\mathrm{Ic}} \sqrt{\frac{1}{g(\mu_{\mathrm{c}})}} \tag{19}$$

6. The toughness correction

The right hand side of the inequality (19) is the critical value $k_{\mathrm{Ic}}^{\mathrm{app}}$ of the apparent stress intensity factor k_{I}, thus:

$$k_{\mathrm{Ic}}^{\mathrm{app}} = k_{\mathrm{Ic}} \sqrt{\frac{1}{g(\mu_{\mathrm{c}})}} \tag{20}$$

This critical value $k_{\mathrm{Ic}}^{\mathrm{app}}$ corresponds to the apparent toughness measured during experiments, as already emphasized in Section 2. The next Figs. 5–8 plot the ratio $k_{\mathrm{Ic}}^{\mathrm{app}}/k_{\mathrm{Ic}}$ for four different materials:

- alumina: $\sigma_{\mathrm{c}} = 220$–$300$ MPa, $k_{\mathrm{Ic}} = 3.8$ MPa $\mathrm{m}^{1/2}$,[1]
- alumina: $\sigma_{\mathrm{c}} = 220$–$300$ MPa, $k_{\mathrm{Ic}} = 2.8$ MPa $\mathrm{m}^{1/2}$,[2]
- silicon carbide: $\sigma_{\mathrm{c}} = 310$–$400$ MPa, $k_{\mathrm{Ic}} = 2.4$ MPa $\mathrm{m}^{1/2}$,[2]
- silicon nitride: $\sigma_{\mathrm{c}} = 400$–$580$ MPa, $k_{\mathrm{Ic}} = 5.4$ MPa $\mathrm{m}^{1/2}$,[2]

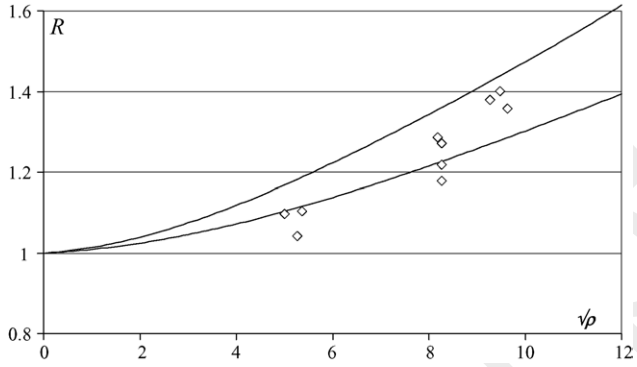

Fig. 6. The ratio $R = k_{\mathrm{Ic}}^{\mathrm{app}}/k_{\mathrm{Ic}}$ vs. the square root of the notch-root radius $\sqrt{\rho}$ ($\mu\mathrm{m}^{1/2}$) for alumina. Diamonds: experiments,[2] solid lines: prediction (20).

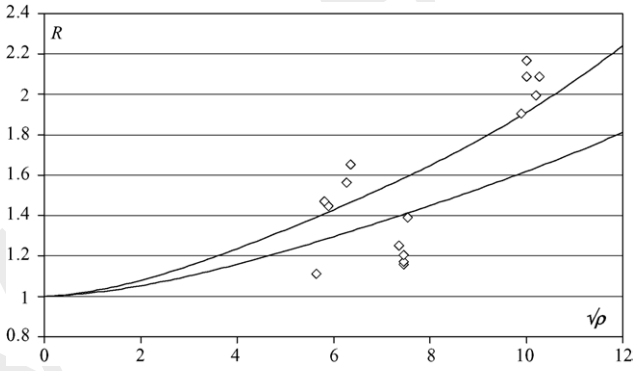

Fig. 7. The ratio $R = k_{\mathrm{Ic}}^{\mathrm{app}}/k_{\mathrm{Ic}}$ vs. the square root of the notch-root radius $\sqrt{\rho}$ ($\mu\mathrm{m}^{1/2}$) for silicon carbide. Diamonds: experiments,[2] solid lines: prediction (20).

and compare the predictions derived from (20) with experiments.[1,2] They show a satisfying agreement (note the different vertical scales) and remain within the scattering due to the experiments. Another cause of some lack of precision is that data are from different sources. Strengths σ_{c} are not provided in the referenced papers,[1,2] they are taken from Internet. The two solid lines in the following figures correspond

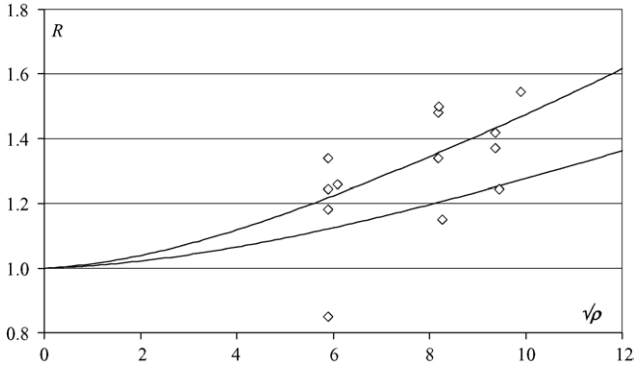

Fig. 8. The ratio $R = k_{\mathrm{Ic}}^{\mathrm{app}}/k_{\mathrm{Ic}}$ vs. the square root of the notch-root radius $\sqrt{\rho}$ ($\mu\mathrm{m}^{1/2}$) for silicon nitride. Diamonds: experiments,[2] solid lines: prediction (20).

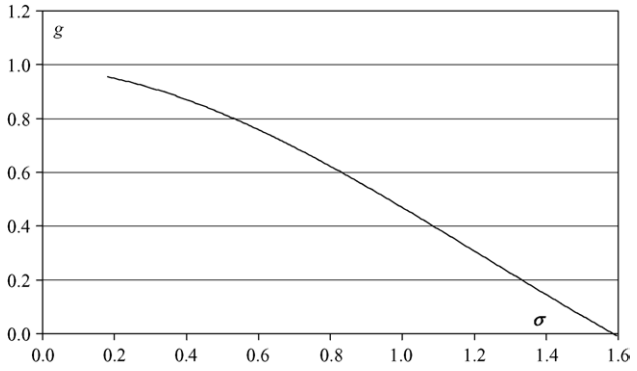

Fig. 9. The implicit representation of functions $\tilde{\sigma}_t$ (horizontal axis) and g (vertical axis).

to the above mentioned strength bounds. The upper lines are associated with the highest strengths.

7. Conclusion

The procedure to determine the actual value of k_{Ic} is the following:

- once the saw cut thickness e, the apparent toughness $k_{\mathrm{Ic}}^{\mathrm{app}}$ and the strength σ_{c} are known,
- solve the following equation derived from (18) and (20), using Fig. 4 to obtain μ_{c}:

$$\tilde{\sigma}_t(\mu_{\mathrm{c}}) = \frac{\sigma_{\mathrm{c}}\sqrt{e}}{k_{\mathrm{Ic}}^{\mathrm{app}}}$$

- determine $g(\mu_{\mathrm{c}})$ using Fig. 3 and compute k_{Ic} from the following relation (see (20)):

$$k_{\mathrm{Ic}} = k_{\mathrm{Ic}}^{\mathrm{app}}\sqrt{g(\mu_{\mathrm{c}})}$$

In these operations μ_{c} is a dummy parameter. The two steps can be resumed to a single one considering the implicit curve derived from Figs. 3 and 4 and plotted in Fig. 9, where $\tilde{\sigma}_t$ and g are respectively in the horizontal and vertical axes. When $\tilde{\sigma}_t$ is known, it provides directly the corresponding value of g.

Alternatively, the above operations can be performed using Table A1 in Appendix A.

This procedure allows bringing a correction to the fracture toughness measurement depending on the notch-root radius, in SENB specimens and for any other test triggering an opening mode at the notch. Only non-symmetric loadings imposing a mixture of symmetric and anti-symmetric modes must be avoided. Applied herein to ceramics, it can be used for any brittle material. The reference curves of Figs. 3 and 4 or Fig. 9 alone are independent of the Young's modulus of the material and it is observed that the Poisson's ratio plays no role. The procedure requires the knowledge of the material strength and the reliability of the final result depends on the accuracy of its determination.

It is often reported that below a given threshold the material is insensitive to the notch-root radius.[1,2] This is mainly due to the fine micro-structure and especially to the grain size in case of ceramics. Of course such a threshold cannot be observed in the present theoretical approach (Figs. 5–8), since the only involved parameters, like the Young's modulus for instance, are macroscopic ones. They average in a sense all the microscopic data. As a consequence, the apparent fracture toughness curves are necessarily smooth from the beginning. Nevertheless, this threshold is about $\rho = 10\ \mu\mathrm{m}$ for the above materials and concerns only the very beginning part of the curves in Figs. 5–8 ($\sqrt{\rho} \leq 3$) while the above correction applies for any (small) notch-root radius. In Figs. 5–8 ρ ranges from $\rho = 0$ to $\rho = 144\ \mu\mathrm{m}$.

Acknowledgements

This work was supported by IFP (Institut Français du Pétrole) under the contract no. CO2351.

Appendix A

See Table A1.

Table A1
The functions $\tilde{\sigma}_t(\mu)$ (17) and $g(\mu)$ (14) vs. the dimensionless length μ

μ	$\tilde{\sigma}_t(\mu)$	$g(\mu)$	μ	$\tilde{\sigma}_t(\mu)$	$g(\mu)$
0.00	1.595	0.000	2.55	0.257	0.933
0.05	1.406	0.127	2.60	0.254	0.934
0.10	1.216	0.293	2.65	0.252	0.935
0.15	1.085	0.411	2.70	0.249	0.935
0.20	0.977	0.497	2.75	0.247	0.936
0.25	0.887	0.562	2.80	0.244	0.937
0.30	0.815	0.613	2.85	0.242	0.938
0.35	0.756	0.654	2.90	0.240	0.938
0.40	0.706	0.687	2.95	0.238	0.939
0.45	0.664	0.715	3.00	0.236	0.940
0.50	0.627	0.738	3.05	0.234	0.941
0.55	0.596	0.758	3.10	0.232	0.941
0.60	0.568	0.775	3.15	0.230	0.942
0.65	0.544	0.790	3.20	0.228	0.942
0.70	0.522	0.803	3.25	0.226	0.943
0.75	0.502	0.814	3.30	0.224	0.943
0.80	0.484	0.824	3.35	0.223	0.944
0.85	0.468	0.833	3.40	0.221	0.944
0.90	0.453	0.841	3.45	0.219	0.945
0.95	0.440	0.849	3.50	0.217	0.945
1.00	0.428	0.855	3.55	0.216	0.946
1.05	0.416	0.861	3.60	0.214	0.946
1.10	0.406	0.867	3.65	0.213	0.946
1.15	0.396	0.872	3.70	0.211	0.947
1.20	0.386	0.876	3.75	0.210	0.947
1.25	0.378	0.881	3.80	0.208	0.947
1.30	0.370	0.885	3.85	0.207	0.948
1.35	0.362	0.888	3.90	0.206	0.948
1.40	0.355	0.892	3.95	0.204	0.948
1.45	0.348	0.895	4.00	0.203	0.948
1.50	0.342	0.898	4.05	0.202	0.949
1.55	0.336	0.901	4.10	0.200	0.949
1.60	0.330	0.903	4.15	0.199	0.949

Table A1 (*Continued*)

μ	$\tilde{\sigma}_t(\mu)$	$g(\mu)$	μ	$\tilde{\sigma}_t(\mu)$	$g(\mu)$
1.65	0.324	0.906	4.20	0.198	0.949
1.70	0.319	0.908	4.25	0.196	0.949
1.75	0.314	0.910	4.30	0.195	0.949
1.80	0.309	0.912	4.35	0.194	0.949
1.85	0.305	0.914	4.40	0.193	0.949
1.90	0.301	0.916	4.45	0.192	0.949
1.95	0.296	0.918	4.50	0.191	0.949
2.00	0.292	0.919	4.55	0.190	0.950
2.05	0.289	0.921	4.60	0.189	0.950
2.10	0.285	0.922	4.65	0.188	0.950
2.15	0.281	0.924	4.70	0.187	0.950
2.20	0.278	0.925	4.75	0.186	0.951
2.25	0.274	0.926	4.80	0.185	0.951
2.30	0.271	0.928	4.85	0.184	0.951
2.35	0.268	0.929	4.90	0.183	0.951
2.40	0.265	0.930	4.95	0.182	0.951
2.45	0.262	0.931	5.00	0.181	0.951
2.50	0.260	0.932			

References

1. Nishida, T. and Hanaki, Y., Effect of notch-root radius on the fracture toughness of a fine-grained alumina. *J. Am. Ceram. Soc.*, 1994, **77**(2), 606–608.
2. Damani, R., Gstrein, R. and Danzer, R , Critical notch-root radius effect in SENB-S fracture toughness testing. *J. Eur. Ceram. Soc.*, 1996, **16**, 695–702.
3. Gogotsi, G. A., Fracture toughness of ceramics and ceramic composites. *Ceram. Int.*, 2003, **29**, 777–784.
4. Leguillon, D. and Yosibash, Z., Crack onset at a v-notch. Influence of the notch tip radius. *Int. J. Fracture*, 2003, **122**(1–2), 1–21.
5. Leguillon, D. and Asymptotic, numerical analysis of a crack branching in non-isotropic materials. *Eur. J. Mech. A/Solids*, 1993, **12**(1), 33–51.
6. Picard, D., Ph.D. thesis in preparation, University P. and M. Curie, Paris 6, France.
7. Leguillon, D., Strength or toughness? A criterion for crack onset at a notch. *Eur. J. Mech. A/Solids*, 2002, **21**, 61–72.